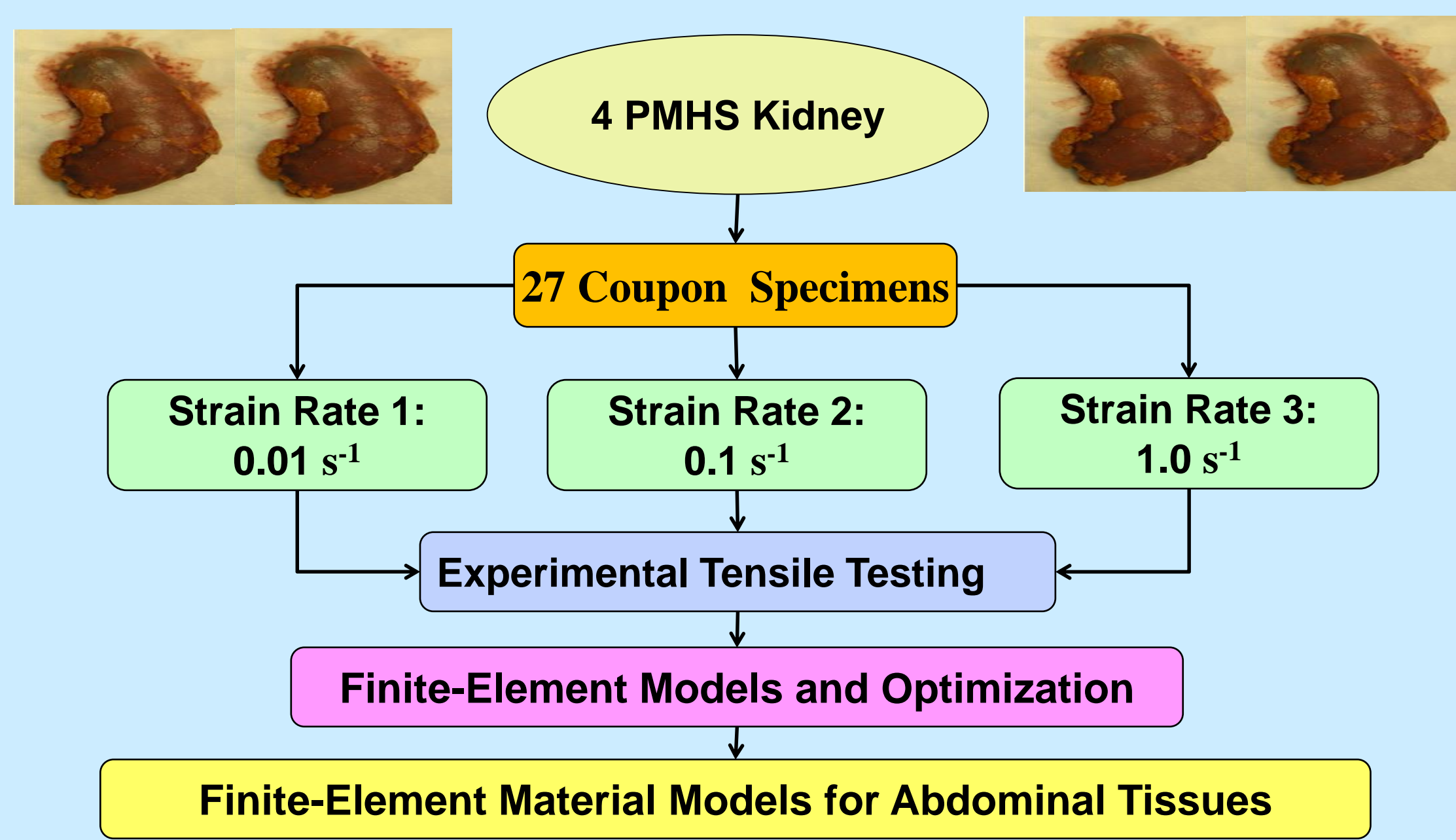


INTRODUCTION

Human finite element (FE) models play an important role in understanding the injury mechanism during a crash and designing advanced restraint systems. However, the accuracy of FE models depends not only on geometrical properties, but also on assigned material and failure models. While various experimental tissue tests of abdominal organs have been conducted, the specimen-specific FE modeling of abdominal organs has rarely been attempted in previous studies and the material models for FE simulation of abdominal tissues are still largely unknown [1-3]. Therefore, the goal of this study was to propose new material and failure models for renal parenchyma and to report the ranges of parameters identified using specimen-specific models.

METHODOLOGY



TESTING PROCEDURE

- Uniaxial tensile tests were performed on 4 PMHS Kidneys
- Coupon specimens (thickness: 5 mm) were cut from the kidneys with a custom blade assembly (Fig. 1-3) and tested within 36 hours after obtaining them.
- Each kidney was divided into three categories which were tested until failure at the following strain rates: 0.01 s^{-1} , 0.1 s^{-1} , and 1.0 s^{-1} .
- A uniaxial load cell was mounted between the linear actuator and the upper clamp (Fig. 3).
- Each specimen was stretched at the two ends, and the time histories of force and displacement were recorded during testing.
- Specimens were immersed in a bath of Dulbecco's Modified Eagle Medium (DMEM) to maintain specimen hydration until test at 98°F .

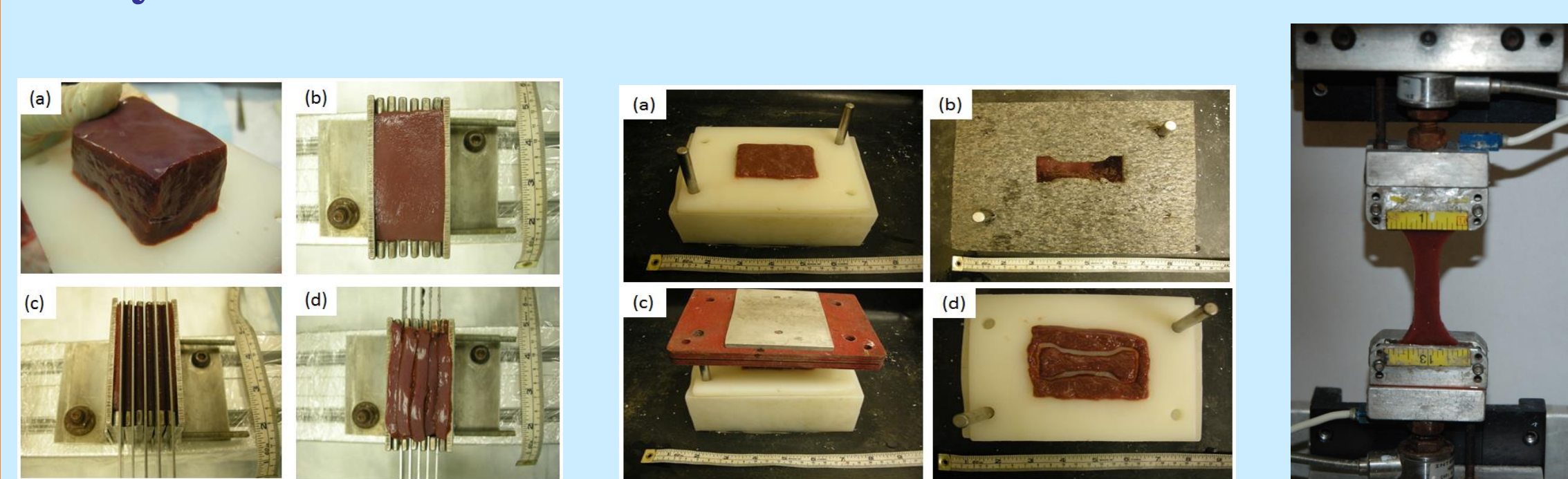


Figure 1: Specimen slicing methodology. Figure 2: Specimen stamping Methodology. Figure 3: Tensile Testing.

Marker & Analytical Analyses

ANALYSIS

- Inertially Compensated Force
 $F_{IC} = F - a * m_{eff}$
 F : measured force
 a : grip acceleration; m_{eff} : effective mass
 - Stretch Ratio $\lambda_1 = \frac{L_n}{L_0}$
 - Incompressibility Constraint: $\lambda_2 = \lambda_3 = \lambda_1^{-1/2}$
 - Green-Lagrange Strain $\epsilon_1 = \frac{1}{2}(\lambda_1^2 - 1)$
 - Ogden- a Hyperelastic Material Model
 $W(\lambda_1) = \mu (\lambda_1^\alpha + 2\lambda_1^{-\alpha/2} - 3) / \alpha$
 $S_1 = \frac{\delta W}{\delta \lambda_1} = \mu (\lambda_1^{\alpha-1} - \lambda_1^{-1-\alpha/2})$; $F_{an} = S_1 A_0$
 - Parameter Identification based on Test data (Excel)
 $\min [F_{error}(\mu, \alpha)]$ where
 $F_{error}(\mu, \alpha) = \sum_{i=0}^n [F_{an_i}(\mu, \alpha) - F_{test_i}]^2$
- α_{an}, μ_{an}

Finite Element Modeling (FEM) and Optimization

- Surface Reconstruction and Meshing (Trugrid) the specimen
-
- Input: Displacement time histories
Variables: μ, α
Output: Force time histories
- FE simulation is run on LS-Dyna to obtain $F_{FE}(t)$
 - Optimization with Successive Response Surface Method (SRSM) using LS-Opt (LSTC, Livermore, CA)
 - Parameter Identification using FE simulations
- $\min [F_{error}(\mu, \alpha)]$ where
 $F_{error}(\mu, \alpha) = \sum_{i=0}^n [F_{FE_i}(\mu, \alpha) - F_{test_i}]^2$
- α_{FE}, μ_{FE}

Cohesive Zone Modeling (CZM)

CZM is an efficient way to model crack propagation within a continuous medium. [5] A Cohesive Zone Layer (CZL) is inserted between two solid adjacent solid elements. Upon simulation, the CZL acts as non-linear spring, softens and fails when the model exceeds a pre-defined fracture energy.

CZM in LS-DYNA® : MAT_186

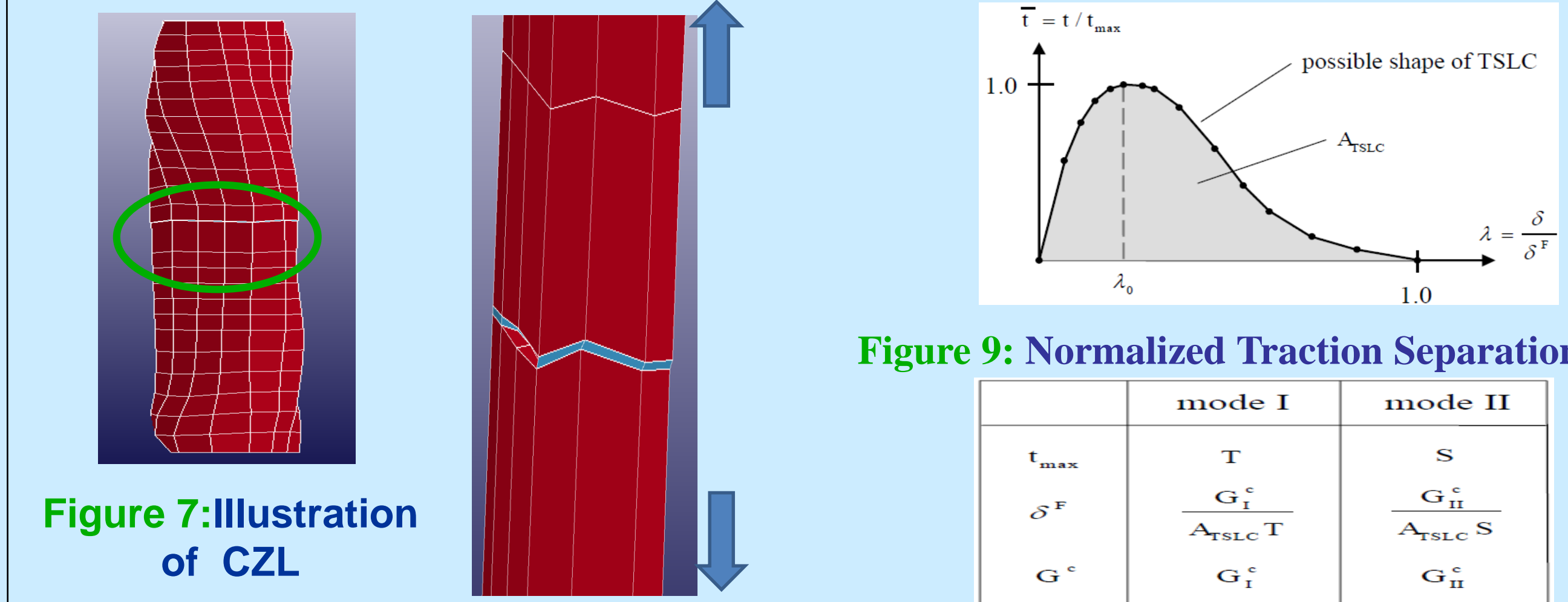


Figure 7: Illustration of CZL

Figure 8: Illustration of CZL Failure

Figure 9: Normalized Traction Separation Law

Figure 10: Parameters used in CZM in LS-Dyna

RESULTS & DISCUSSION

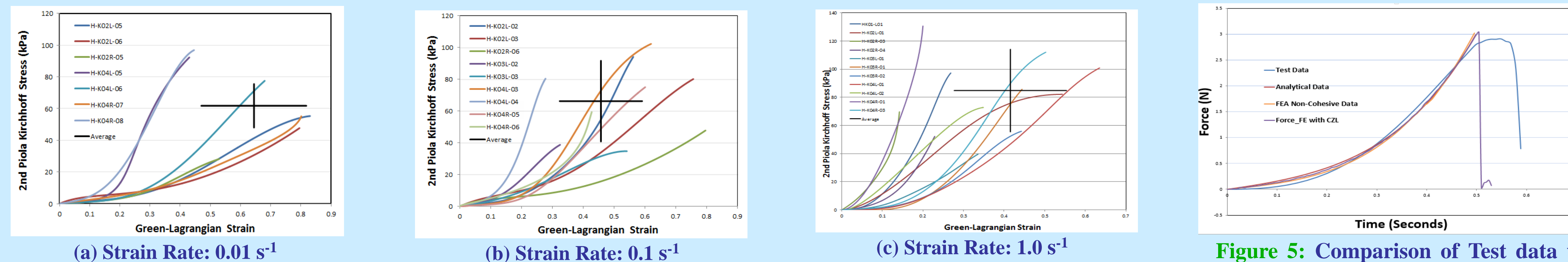


Figure 4: Second Piola-Kirchhoff stress vs. Green-Lagrangian strain curves tensile testing by loading rate (Marker Data).

Figure 5: Comparison of Test data vs. Analytical vs. FE vs CZM for Rate-3

Rate	# of Specimens	Desired Strain Rate (s^{-1})	Average Strain Rate (s^{-1})	Average Failure Strain	Average Failure Stress (kPa)
Rate 1	7	0.01	0.007 (± 0.001)	0.645 (± 0.174)	61.735 (± 13.708)
Rate 2	9	0.1	0.073 (± 0.020)	0.457 (± 0.1334)	66.142 (± 25.372)
Rate 3	11	1.0	0.704 (± 0.121)	0.415 (± 0.138)	84.783 (± 29.292)

Table 1. Averages and standard deviations of measured strain rate, failure strain and failure stress by loading rate (Marker Data).

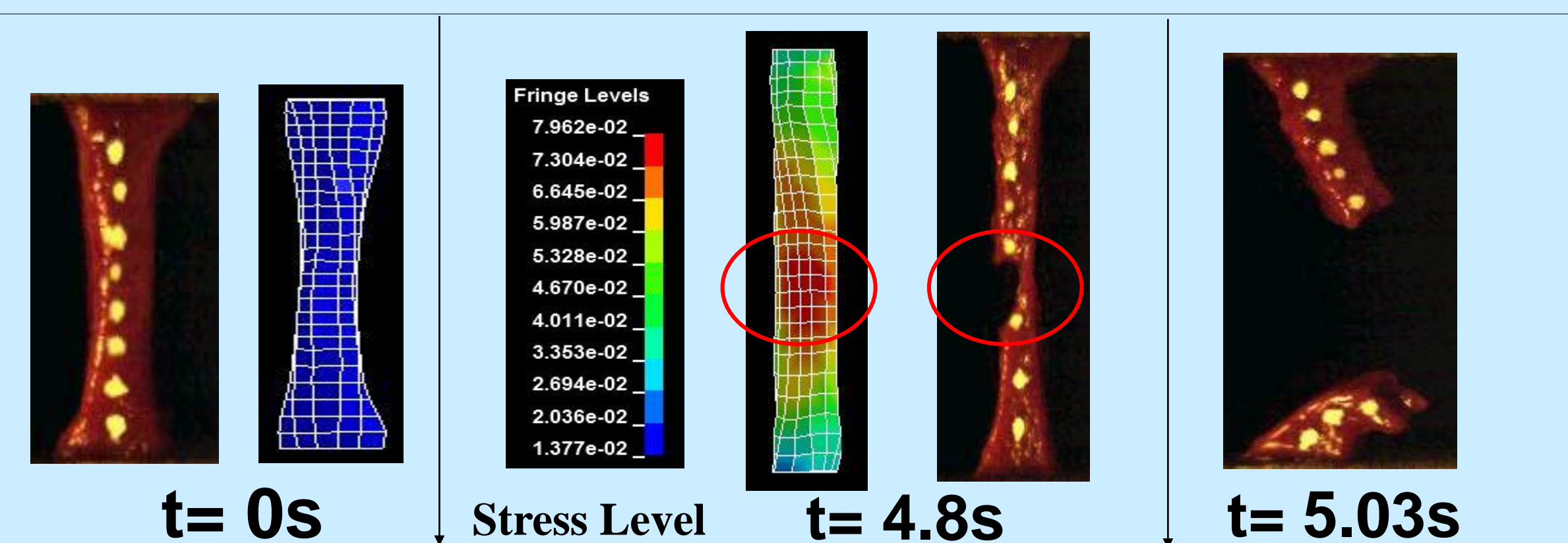


Figure 6: The comparison between video data and simulated results for a specimen at 1/s load rate. The failure location was highlighted in both the test and simulation

Rate	μ_{an} (kPa)	α_{an}	μ_{FE} (kPa)	α_{FE}
Rate 3	8.24	9.683	3.963	11.655

Table 2: Ogden Material Properties obtained from Analytical and FE Modeling – Rate 3 specimen

- The current study quantifies the material response of PMHS human kidney parenchyma in tensile loading at various loading rates.
- The data from this study shows that the response of parenchyma is non-linear, and exhibits visco-elasticity under tensile loading.
- An Ogden hyper-elastic material model approximates reasonable the parenchyma response in tension.
- The FE models with parameters identified by FE approach showed a closer response to the test data. The models with parameters identified by analytical approach showed a stiffer response.
- With increased loading rate, the failure stress increased while the failure strain slightly decrease.
- The rate dependence of kidney parenchyma should be taken into account when developing material models or injury thresholds.
- Cohesive Zone Model showed promising results for modeling the failure and post-failure behavior of the parenchyma

FUTURE WORK

- Compute $\mu_{an}, \alpha_{an}; \mu_{FE}, \alpha_{FE}$ values of all tested kidney specimens & calculate corridor data corresponding to the three strain rates.
- Cohesive Zone Layers will be inserted along both longitudinal & horizontal axes of the FE model of Kidney as shown in Figure:11
- Efforts will be made to extract specimen specific Cohesive Zone Parameters through a blend of Finite-Element-Modeling and Optimization approach.
- It is believed that the methodology developed will be extended in the future to develop more accurate material and failure models of abdominal organs, which consequently will result in more accurate FE human models.



Figure 11: Cohesive Zone Layers are represented as thick blue structures for clarity

REFERENCES

- Kemper, A.R., Santiago, A.C., Stitzel, J.D., Sparks, J.L., Duma, S.M., 2012. Biomechanical response of human spleen in tensile loading. Journal of Biomechanics 45(2), 348-355.
- Kemper, A.R., Santiago, A.C., Stitzel, J.D., Sparks, J.L., Duma, S.M., 2010. Biomechanical response of human liver in tensile loading. Annals of Advances in Automotive Medicine 50, 15-26.
- Snedeker, J.G., Niederer, P., Schmidlin, F.R., Farshad, M., Demetropoulos, C.K., Lee, J.B., Yang, K.H., 2005. Strain-rate dependent material properties of the porcine and human kidney capsule. Journal of Biomechanics 38(5), 1011-1021.
- Hu, J., Klinich, K.D., Miller, C.S., Nazmi, G., Pearlman, M.D., Schneider, L.W., Rupp, J.D., 2009. Quantifying dynamic mechanical properties of human placenta tissue using optimization techniques with specimen-specific finite-element models. Journal of Biomechanics 42(15), 2528-2534.
- Makhecha DP. Dynamic fracture of adhesively bonded composite structures using cohesive zone models. Ph.D. dissertation, Virginia Polytechnic Institute and State University, Blacksburg, VA; 2005.
- Mat_186, LS-DYNA® Keyword User's Manual Volume II: Material Models, 2012.